A Wearable Sensing System for Tracking and Monitoring of Functional Arm Movement

Kim Doang Nguyen, *Student Member, IEEE*, I-Ming Chen, *Senior Member, IEEE*, Zhiqiang Luo, *Member, IEEE*, Song Huat Yeo, and Henry Been-Lirn Duh, *Senior Member, IEEE*

***Abstract*—This paper presents a new sensing system for home-based rehabilitation based on optical linear encoder (OLE), in which the motion of an optical encoder on a code strip is converted to the limb joints' goniometric data. A body sensing module was designed, integrating the OLE and an accelerometer. A sensor network of three sensing modules was established via controller area network bus to capture human arm motion. Experiments were carried out to compare the performance of the OLE module with that of commercial motion capture systems such as electrogoniometers and fiber-optic sensors. The results show that the inexpensive and simple-design OLE's performance is comparable to that of expensive systems. Moreover, a statistical study was conducted to confirm the repeatability and reliability of the sensing system. The OLE-based system has strong potential as an inexpensive tool for motion capture and arm-function evaluation for short-term as well as long-term home-based monitoring.**

***Index Terms*—Motion capture and analysis, wearable sensors.**

I. Introduction and Motivation

RECENT evidence has demonstrated that intensive massed and repeated practice is effective for recovery of functional motor skills [1]. Rehabilitative therapy is essential to the treatment process for helping accident (such as stroke) survivors to regain their limb functions as much as possible. The most common objective of rehabilitation is to achieve a level of physical and psychological functioning that allows patients to return home and perform everyday activities. Rehabilitation exercises are specifically designed to match the goals of each individual. Study in [2] showed that the trajectories of upper extremity of stroke patients are characterized by increased movement variability, increased motion segmentation, and spatial and temporal incoordination in comparison with healthy people. In addition, recovery from stroke has strong correlation with the smoothness of upper extremity motion [3]. Upper limb motor recovery during rehabilitation can be also improved by the iterative training of simple, isolated, and single joint movements [4], [5]. During rehabilitation, doctors would like to assess human body gestures in order to perceive joint motion during activities of daily living in patients with movement disorder. Examination on the performance of their upper limb motion, when patients do simple tasks, is crucial in effectively designing and appraising rehabilitation therapy and treatments for upper limb movement disorders [6].

A general aim of this study is to design a home-based rehabilitation system to assist the motor recovery of upper limb during the process of stroke rehabilitation. Traditionally, neurorehabilitation techniques require intensive, subjective and supervised assessment of motor function, and therapeutic procedures monitored by a medical professional for each patient. Rehabilitation interfaces based on motion tracking technologies enable customizable and automatic therapy, quantitative examination of patient performance. Compared to traditional neurorehabilitation methods, they offer better specificity, sensitivity, resolution, repeatability, and reliability. However, bringing rehabilitation sessions to the home environment still remains a challenge [7].

Motion analysis in rehabilitation is performed by measuring human-body kinematics by employing motion capture systems, including optical, inertial/magnetic unit (IMU), electrogoniometer, and mechanical tracking. However, the technologies' disadvantages make them unsatisfactory for long-term human movement monitoring in home-based rehabilitation. Despite their accuracy, optical systems are not only the most expensive capture systems, but also require complicated setup, calibration, and data processing. Moreover, they suffer from occlusion, lack of portability, and user's inconvenience caused by the large number of markers [8]. Also, though optical systems are used for gait and posture analysis of entire body, it is hardly used in functional assessment of a single joint or certain body part. The drawbacks of IMU-based tracking system include limited field of operation, accumulated errors (gyroscope), high sensitivity to disturbances by metallic objects (magnetic sensor), excessive sensor fusion, and high-power consumption [8]. Though electrogoniometers are used to measure joint angle, they need careful sensor alignment and calibration for accurate results and may restrict movements if many of them are used. Therefore, it is difficult to use these devices at home for long periods. Mechanical tracking systems have poor wearability and portability, and fail to satisfy safety requirements for personal use due to the presence of mechanical parts in movement. Also, ground-based systems require confine work spaces [9]. Rotary encoders in exoskeletons have problems with alignment of rotation centers, which worsen tracking accuracy from time to time. Thus, mechanical capture systems are not suitable for home environment.

The goal of this paper is therefore to design a new motion capture system for continuous monitoring of human arm

Manuscript received May 27, 2009; revised September 22, 2009 and November 22, 2009; accepted December 2, 2009. Date of publication February 8, 2010; date of current version January 19, 2011. Recommended by Technical Editor V. N. Krovi. This work was supported in part by the Agency for Science, Technology, and Research under Science and Engineering Research Council Grant 0521180050 and in part by the Media Development Authority, Singapore, under National Research Foundation Grant IDM004–005.

K. D. Nguyen, I-M. Chen, Z. Luo, and S. H. Yeo are with the School of Mechanical and Aerospace Engineering, Nanyang Technological University, Singapore 639798 (e-mail: kdnguyen@ntu.edu.sg; michen@ntu.edu.sg; zqluo@ntu.edu.sg; myeosh@ntu.edu.sg).

H. B.-L. Duh is with the Department of Electrical and Computer Engineering, National University of Singapore, Singapore 117574 (e-mail: eledbl@nus.edu.sg).

Color versions of one or more of the figures in this paper are available online at http://ieeexplore.ieee.org.

Digital Object Identifier 10.1109/TMECH.2009.2039222

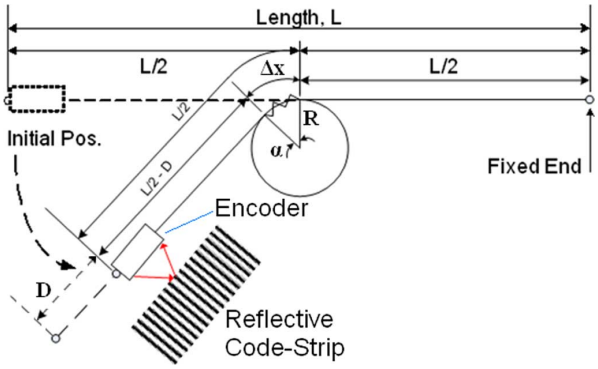

Fig. 1. OLE working principle—conversion of displacement to angle.

movement based on the concept of an optical linear encoder (OLE) [10] that is nonintrusive, noncumbersome, and compact enough to be embedded into clothes while retaining comfort. The system captures the linear and orientation information from sensing modules placed on the human body. Linear information, which is provided by the OLE wrapping around joints, is utilized to estimate joint angles. Microelectromechanical systems (MEMS) based accelerometers provide acceleration and orientation of links on which the sensing modules are attached. The fusion of an accelerometer with the new OLE provides a complete system, which is able to track link's orientations, accelerations, and joint angles. A sensor network of three such sensing modules is connected by controller area network (CAN) bus to track the arm movement. The low cost, wearability, and portability of the sensor network allow extended home monitoring of patients under rehabilitation. The wearable system can be donned, doffed, and operated everyday without close supervision of medical professionals.

II. Goniometry Based on OLE

A. Working Principle

The OLE includes an infrared emitter and a receiver built in a single package [11]. The infrared light from the emitter is reflected off a reflective code strip, on which parallel lines, which are 0.1 mm apart, were engraved. In operation, the encoder counts the number of lines it has passed upon the strip, which can be converted to travel distance with direction index. Therefore, the code strip, together with the emitter and the receiver, form a precise distance-measurement device of 0.1 mm resolution.

In order to obtain the joint angle of a human joint (e.g., elbow), the linear encoder is attached to a wire that is fixed to one side of the joint (i.e., forearm), while the linear encoder assembly is fixed to the upper arm. The linear encoder is free to slide along its longitudinal axis, which is coincident with the single free axis of the wire. When used, the linear encoder is attached to the body skin. The sensor is wrapped around the joint. Because the center of rotation of the joint is within the skeleton structure and not on the surface of the limb segment, the offset from the sensor placement to the joint rotation center will enable us to interpret the joint displacement by the linear displacement of the sensor reading, as shown in Fig. 1. We assume that the stretch caused by the elbow bend produces a linear displacement D (provided by the encoder readings). Also, we assume that the radius of the offset disk formed due to the sensor placement is R. The sensor displacement due to the joint bending along the disk Δx is therefore equal to D.

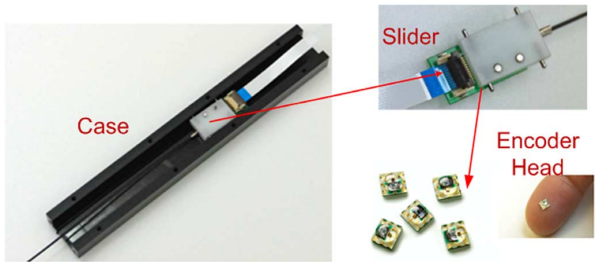

Fig. 2. OLE mechanical design: the slider moves upon the case as the encoder counts the number of lines based on reflected signals from the code strip.

We have

$$\Delta x = \frac{\alpha}{360^\circ} 2\pi R. \tag{1}$$

Therefore,

$$\alpha = \frac{D}{R} \frac{360^\circ}{2\pi}. \tag{2}$$

Biometric data, such as bone length and structure and skin characteristics, alter from person to person. This variation affects the accuracy and reliability of motion capture process. Therefore, a scale factor (SF) is inserted into the (2) to compensate for biometric effects, thus disturbing the tracking as

$$\alpha = \mathrm{SF}\,(D_c)\, \frac{D}{R} \frac{360^\circ}{2\pi}. \tag{3}$$

$\mathrm{SF}\,(D_c)$ is a function of calibrating joint angle D_c

$$\mathrm{SF}\,(D_c) = 2\pi \frac{\alpha_c}{360^\circ} \frac{R}{D_c}. \tag{4}$$

The SF is obtained through a calibrating process, which is as follows.

1) Joint poses predefined gestures (0°, 30°, 60°, 90°, etc.).
2) D_c, the distance travelled by the encoder, is recorded from the OLE readings.
3) SF(D_c) is computed by (4), with known α_c and D_c.
4) Thus, when using (3) to calculate the actual joint angle, any arbitrary set (D, SF) is interpolated from the calibration points defined by (D_c, SF_c).

B. Mechanical Design

A miniature linear encoder is made to slide over a Delrin base structure, as depicted in Fig. 2. The encoder is attached to a flexible stainless-steel wire that has a diameter of 1 mm. It is guided by a Teflon tube to restrict it to 1 DOF. The code strip is adhered to the case, whose function is to allow the encoder to travel above the linear code strip while maintaining a constant gap of 0.4 mm between the code strip and encoder.

III. Body Sensor Network

A. Sensing Module

The wearable sensing module is self-contained and consists of an OLE, an accelerometer, a digital signal controller, and a

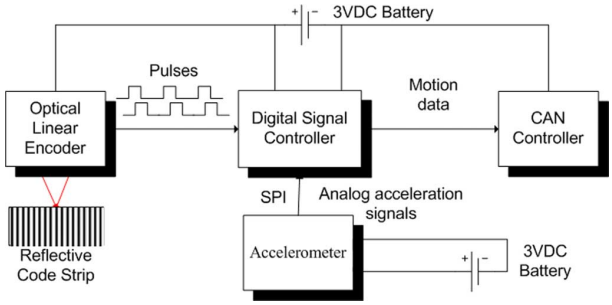

Fig. 3. Block diagram of the sensing module.

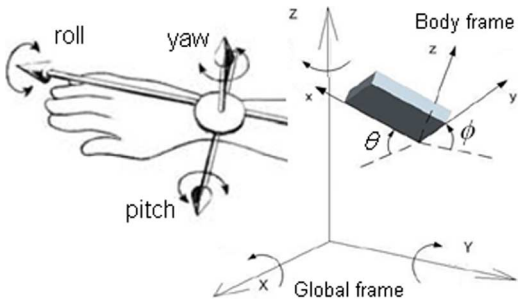

Fig. 4. Coordinate frames (body and global) and roll-pitch-yaw angle.

CAN controller. The sensing module's electrical block diagram is shown in Fig. 3. The OLE measures the angle of the joint it wraps around. The accelerometer gives the link's orientations on which the sensing module is mounted. In the accelerometer's static condition, the gravity vector is composed of the three orthogonal accelerations [12]. Hence,

$$\theta = \sin^{-1}\left(\frac{a_X}{g}\right), \text{ and } \phi = \sin^{-1}\left(\frac{a_Y}{g\cos\theta}\right) \qquad (5)$$

where $[a_X\ a_Y\ a_Z]^{\mathrm{T}}$ is gravity vector measured in its local coordinate, θ and φ are pitch and roll angles in the global coordinate, respectively (see Fig. 4). Yaw angle cannot be measured by the accelerometer.

B. Sensor Network

To capture the motion of human arm, three sensing modules and a data concentrator (DC) are connected to form a sensor network, in which all communications among the sensor nodes and the DC are performed by CAN bus, as illustrated in Fig. 5. The modules are connected to the bus in a daisy-chain fashion: if the bus is driven to a logical 0 by just one node, then the whole bus is in that state regardless of the fact that other nodes are transmitting either a logical 1 or 0. All nodes have the common component structure. The microprocessor operates the embedded program, which constantly polls the analog signal from the accelerometer and the digital signal from the OLE, and then, queue the combined message via serial peripheral interface bus (SPI) port to the CAN controller, handling transmitting, receiving, and filtering of packets of useful information. The DC acts as a gateway to communicate with other devices as well as the master that control the behaviors of sensor nodes. In our sensor network, CAN bus plays as a broadcast type of bus, in which all nodes can "hear" all transmissions. Using a message filter in nodes' firmware, each node only responds to

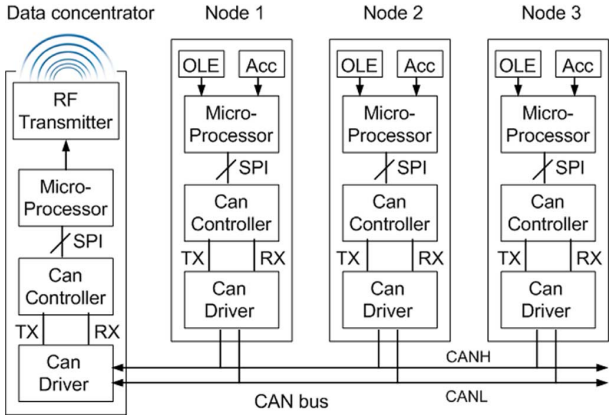

Fig. 5. Motion-capture sensor-network block diagram.

a specific message. Data acquisition starts as the PC sends to the DC a request with the following structure:

<type> <location> <nodeID>.

The request specifies data type, node location, and ID. The DC in turn collects the respective information from the interested nodes via the CAN bus, and then sends back to the PC, by a wireless transmitter, with the following message structure:

<type> <location> <nodeID> <encoder> <X> <Y> <Z>.

The reply includes the configuration information, the respective encoder readings, and the accelerations along *x*-, *y*-, and *z*-axes of the accelerometer. The entire transmitting process is synchronized by the standard CAN protocol.

An RF station is designed to get motion data from the sensor network via universal serial bus (USB) ports. The RF station runs with TinyOS operating system for wireless networks. Communication between the RF station and the DC is established by ZigBee protocol. Handshaking is controlled by the media access control (MAC) layer defined by IEEE 802.15.4 standard.

IV. Sensor Placement and Package Design

A. Placement of OLEs on Human Arm

This proposes a placement scheme for the sensing modules on the arm based on its biomechanics and bone structure.

1) Shoulder Joint: The glenohumeral joint, which is the shoulder's major joint, is a ball-and-socket joint that allows the arm to rotate or to hinge out and up away from the body and around it. The sensor can be fixed on the upper arm, while the fixed end is placed at the top of acromial arch, as shown in Fig. 6 (left). When the upper arm ab/adducts, the sensor will move relatively to the fixed end, therefore, give the data indicating the angle of movement. The upper arm flexion/extension and in/external rotation are tracked by the accelerometer of the same sensor node.

2) Elbow Joint: The elbow joint is a ginglymus or hinge joint, a 1-DOF joint. Placement of the sensor for the elbow is: the fixed cable end point is placed as reference point on the upper arm, while the OLE is placed on the forearm, as depicted in Fig. 6 (middle). The pulling wire is ensured to pass through the olecranon, so that the OLE responds most sensitively to the elbow flexion.

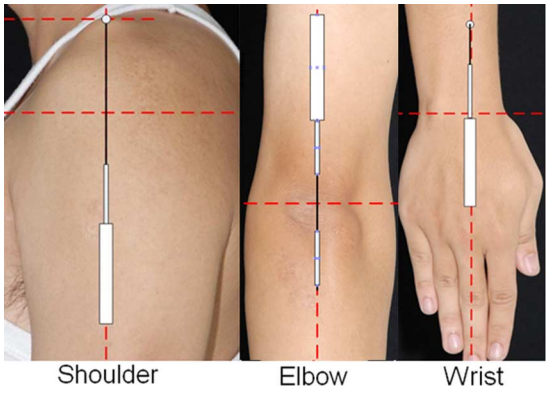

Fig. 6. Placement of the OLEs on shoulder, elbow, and wrist joints.

3) Wrist Joint: The narrow-range motion of wrist poses as a problem of tracking systems, especially for optical and ultrasound sensors, as they are unable to differentiate between the positions of the two markers that are closely placed together. To capture the wrist flexion and hyperextension, the OLE is attached on the back of the hand, and the fixed cable end point is on the forearm, see Fig. 6 (right). When the wrist flexes, the encoder moves upon the code strip. The encoder's travel distance is converted into the wrist flexion/extension. The wrist deviation and pro/supination are tracked by the node's accelerometer.

B. Sensor Package Design

When designing the package for holding sensors on the human arm, the following criteria are required.

1) The sensor package places the sensors on human arm, according to the placement in the previous section.
2) The sensor unit and the pulling cable's tip are fixed at two sides of the joint, so that the OLE can accurately measure the joint movement.
3) The design is comfortable without slipping on users' skin.
4) The sensor package should be easy to wear by one person and fit to human arms with different size.
5) The package does not restrain the human movement.

Based on these criteria, we designed a modular-based fabric suit to package sensors in this study.

1) Shoulder Module: As in Fig. 7(a), the shoulder module composes of one sensor and the concentrator used in the CAN bus. The entire sensor is covered by fabric for aesthetic purpose. A pouch is located near the fixed end of the guiding strip to house the battery pack. On the inner side of the clothing unit for shoulder joint, the point that users are asked to put at their acromion process. The pulling wire is also aligned along the line crossing this shoulder process, as shown in Fig. 6 (left).

2) Elbow Module: The elbow module also holds one sensor at one side and locks the tip of the guiding strip at another side [see Fig. 7(b)]. At both sides, the Velcro straps are used to fix the module on the upper arm and the forearm. Furthermore, the sensor and wires are covered by the fabric housing. The elbow fabric module is marked at the point at which users' olecranon process coincides. Also, the pulling wire must be aligned along the line passing this elbow process (see Fig. 6, middle).

3) Wrist Module: The wrist sensor is mounted on a Velcro strip to ease replacement and adjustment of its position [see Fig. 7(c)]. The guiding strip is then covered by a layer of extension of the fabric to secure the path of motion of the guiding strip and also for aesthetic purposes. The fixed end used to secure the tip of the guiding strip is also covered by another piece of fabric of the same textile. On the inner side of the clothing module for wrist joint, the positions where users are supposed to put their radial and ulnar styloid processes are marked. This together with the guide to align the pulling wire along the bisector between the styloid processes (see Fig. 6, right) make the user can do only one way in the module every time.

Fig. 7. Sensor package design for shoulder, elbow, and wrist. (a) Shoulder. (b) Elbow. (c) Wrist.

V. Experimental Results of Comparison Tests

To assess the OLE's performance as well as the sensor network as a motion capture system, we conducted a variety of comparison experiments. The first set of tests was conducted to evaluate the accuracy of the OLE in ideal condition, with rigid joint and link, actuated by PowerCube. The second set compared OLE's performance for the arm flexion with BIOPAC Goniometer and Measurand ShapeWrap.

A. Repeatability and Accuracy Test of OLE

This experiment verifies the accuracy and repeatability of OLE compared with an accurate rotary system, PowerCube. The sensing module was mounted onto a jig that is attached to a PowerCube [see Fig. 8(a)]. This PowerCube rotary module has a 2000-pulse per revolution encoder, which means 0.18°/pulse. Displacement results from the linear encoder were taken while the rotary module was rotated from 0° to 90° at intervals of 10°. The readouts from the linear encoder, converted to degree using (2), were plotted against Powercube's rotation. Fig. 8(b) illustrates a linear relationship with a correlation coefficient of 0.99 and rms error of 1.2° between the two systems. The

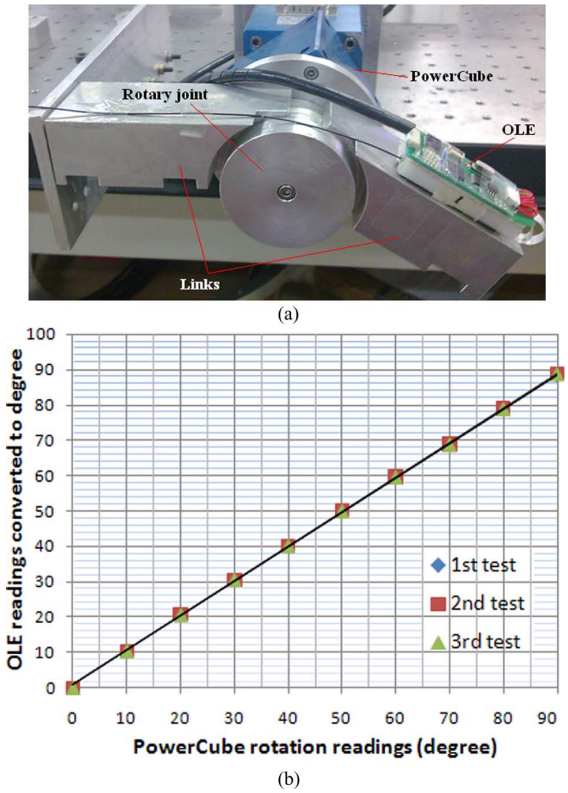

Fig. 8 (a). Setup for the PowerCube experiment. (b) OLE measurements with respect to PowerCube readings.

results confirm the OLE's working principle in (2) as well as its repeatability and accuracy.

B. *In Situ* Test of OLE Sensors

These *in situ* tests aim to examine the OLE performance while recording actual human motion against two popular motion capture systems, electrogoniometer, and ShapeWrap. The electrogoniometer measures the orientation difference of two links of a joint via change of resistance in a set of strain gauges. ShapeWrap records joint angle using fiber optics. Fig. 9(a) shows the experimental setup. Three healthy male subjects performed two sets of experiments each to test the sensor's accuracy versus the two benchmark systems. In the first experiment, each subject was asked to perform normal repeated bending of his elbow (about 0.6 Hz). The second experiment required him to repeatedly flex his elbow as fast as possible (2 Hz). Fig. 9(b) (c) illustrates the readings of the OLE as compared to that of Goniometer and ShapeWrap for the first and the second experiment, respectively. Statistical analyses of the performance and error between OLE and the two systems show that the average rms error of OLE versus Goniometer is 3.8° with the average correlation coefficient of 0.990; and the average rms error of OLE versus ShapeWrap is 3.1° with the average correlation coefficient of 0.992.

VI. Experimental Results of Statistical Tests

In addition to the validation of the OLE sensor as a new way of measuring body joint movements, further tests were carried out to use multiple OLE-based sensing modules as a body motion

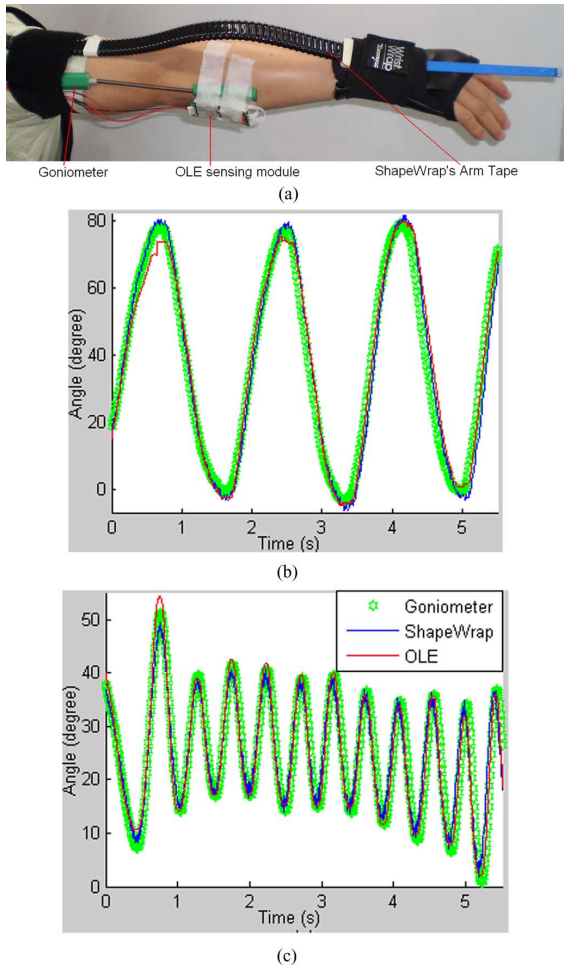

Fig. 9. (a) Three motion capture system on human arm for the comparison test. (b) Results for normal bending of elbow (about 0.6 Hz). (c) Results for high-frequency flexion (about 2 Hz).

capture system. The repeatability and reliability of OLE-based wearable sensor network were tested for *in situ* experiments. The configuration of OLE-based system for this experiment is a single arm version with a wrist, elbow, and shoulder module, as shown in Fig. 10. The experimental procedure is adapted from a therapy session of stroke rehabilitation. The objective of the experiments is to testify the repeatability and reliability of the entire OLE-based motion capture system.

A. *Experimental Procedures*

Five subjects were asked to perform a reaching task to assess the system's repeatability. Subjects, wearing the arm suit, drove the virtual arm to reach a virtual ball in the simulation environment. The virtual ball was controlled to move in predefined route to guide both the real and virtual arm movements, as shown in Fig. 10. In fact, the test is similar to a virtual rehabilitation session. The procedure is as follows: 1) the arm first lifts up; 2) when the shoulder pitches to the maximal angle, the elbow starts bending to the maximal angle and then returns; 3) when the forearm and upper arm lie in one line, the wrist starts bending to the maximal angle and then returns; and 4) the wrist starts rolling to touch ball and then back; after that,

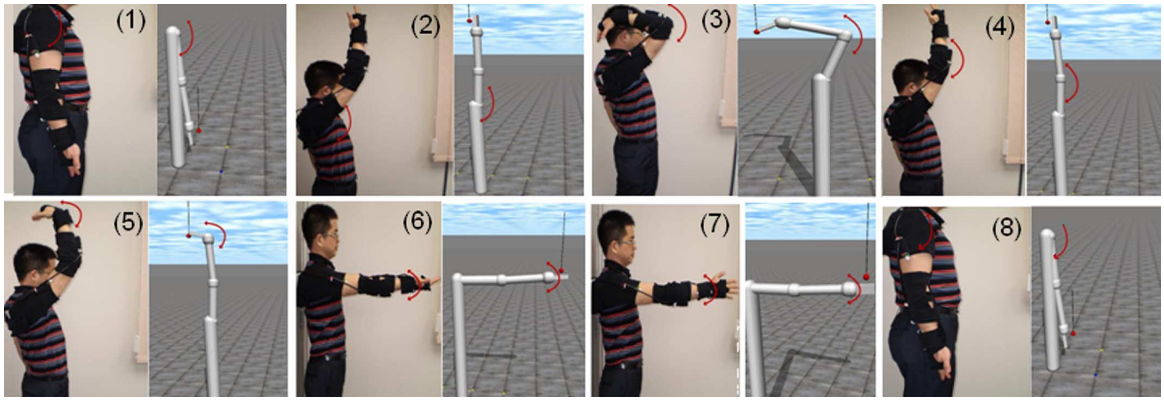

Fig. 10. Arm movement testing procedure: (1) initial gesture, (2) lift arm as vertical as possible, (3) bend elbow backward, (4) return to the gesture in (2), (5) bend wrist backward, then return to the gesture in (2), (6) move the arm to horizontal gesture, (7) roll the wrist and then move back, and (8) return to the gesture in (1).

the whole arm returns to the initial position. All three joints, shoulder, elbow, and wrist needed to rotate from the rest state to the maximum tension and then return. Each subject performed the arm-reaching task for ten trials.

B. Analysis

1) Repeatability Testing: Each raw data file (one subject) contained one data block of ten trials of reaching the ball. For each of the ten trials, sensors captured four DOFs of arm movements, including shoulder flexion, elbow, wrist flexion, and wrist rotation. And, each DOF was collected with 1000 sample data during the reaching task. Therefore, the reaching task performed by each subject can be represented by a 3-D array of data $\{X_{ijk}\}$, $i = 1, \ldots, 10$, $j = 1, \ldots, 10$, and $k = 1, \ldots, 4$ to specify the ith position in the jth trial (subject) for the kth DOF. The maximum and minimum trial data averages were used to establish the range of each DOF. The range is computed by

$$R_k = \max_j \overline{X}_{jk} - \min_j \overline{X}_{jk} \tag{6}$$

where

$$\overline{X}_{jk} = \frac{1}{10} \sum_{i=1}^{10} X_{ijk}. \tag{7}$$

From individual data block ranges (R_k) and corresponding standard deviations (SDs) of the X_{jk} values, an overall value of average range and SD across all five subjects was computed. Data processing was performed in SPSS.

2) Reliability Analysis: Reliability analysis was conducted by computing an intraclass coefficient (ICC) to identify the source of variability between measures. ICC values close to one that indicate high internal consistency in the measurement method, thus giving confidence that the test results reflect true scores. Reliability analyses were performed by randomly selecting two of the ten data blocks per subject, and further, randomly selecting one of the ten trials within each data block, and then, ICC was computed for the two trials in SPSS. This was repeated 20 times.

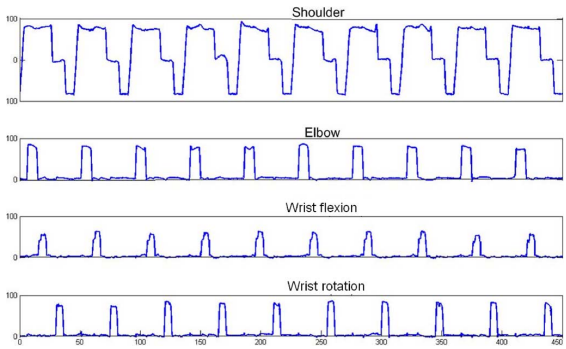

Fig. 11. Raw data from each joint for a single data block (one subject) collected during the performance of the arm-reaching task. Angles (the vertical dimension) are in degrees. Time (the horizontal dimension) is in seconds. When the arm lies horizontally, the degree of the shoulder joint is 0°. When the upper arm, forearm and hand lie in one line, the angles of both elbow and wrist (bend) are 0°. Wrist roll is the relative angle of the hand with respect to the forearm.

C. Results

1) Repeatability: A single data block containing ten trials of performing the arm-reaching task is shown in Fig. 11. It should be noted that the angle of the shoulder joint was coded to range from −90° to 90°. Each block produced four average values for our sensors. Five data blocks were processed to produce five average values for each DOF (see Fig. 12). The average error range is 2.819° (average of range shown in Fig. 13). In addition, the average SD is 0.697° (average of SD shown in Fig. 13).

2) Reliability: Reliability analysis showed high ICC values for all channels within 0.959–0.975, with an overall average of 0.967 (see Table I), showing our system's ability to perform and maintain its functions in routine tasks, with different biometric subjects.

VII. Discussion

The use of motion capture technologies has revolutionized variety of disciplines, ranging from medicine, healthcare to entertainment. However, most current motion tracking systems require inflexibly confine working spaces. This hinders the widespread latitude of using motion capture in inexpensive applications. According to the review in [13], current motion capture systems are far from the ideal tracker-on-a-chip. Also, there

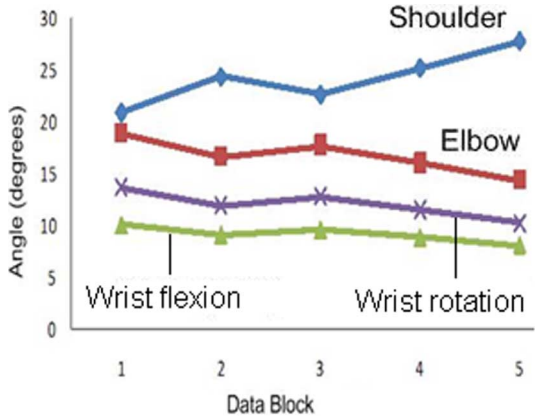

Fig. 12. Individual data block averages for repeatability. Each value is the average of ten cycles of the arm-reaching task for each DOF per subject.

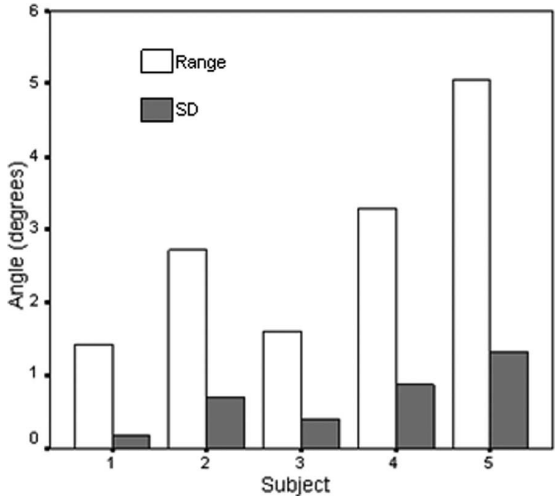

Fig. 13. Average range and SD for each subject.

TABLE I
INTRACLASS CORRELATION COEFFICIENT OF RELIABILITY

Shoulder	Elbow	Wrist (bend)	Wrist (roll)	Average
0.975	0.974	0.959	0.962	0.967

are few sensing technologies, while algorithms that edit, transform, interpolate, and recompose motion data are abundant. The range of motion capture technologies used in rehabilitation is even more limited.

Our system is the first tracking system that uses OLEs and the combination of OLEs and accelerometers to perform the task of motion capture. The simplicity in technology allows us to minimize the production cost (cost of OLE + accelerometer + microcontroller + circuit and mechanical design is approximately (USD) \$10 + \$15 + \$5 + \$10 = \$40, respectively). Besides the low cost, our system has certain advantages over other motion tracking technologies used in rehabilitation. Compared with IMU, OLE does not suffer from data drift due to the integration of angular velocity (gyroscope) and analog–digital converter (ADC) resolution errors, platform tilt errors, geomagnetic variation, and nearby ferrous distortions (magnetic sensor). Quadrature digital signals from the OLE and acceleration data from the accelerometer do not require excessive sensor fusion algorithms, such as extended Kalman filter normally used in IMU. In addition, the OLE directly captures the joint angle. Therefore, only one OLE is needed for individual joint assessment, while two IMUs are requisite for the same purpose. OLEs do not suffer from the difficulties in center-of-rotation alignment of rotary encoder (widely used in exoskeleton). OLEs are basically aligned along the plane, where skin is stretched the most when the joint is moving. The detailed guide for OLE placement is discussed in Section IV. Moreover, compared with exoskeleton, OLE is simple in design, easy to wear, and has compact package. Our sensor network works without a restrictive work space. The current wireless protocol allows users to move freely in a region of 10 m radius, which can be much extended with Bluetooth.

Admittedly, the best-reconstructed human motion data are still not perfect. The OLE-based module is not able to capture the horizontal movement of the upper arm. The reason is that each OLE can capture only 1 DOF, while the accelerometer cannot track its yaw. The problem can be completely resolved by replacing the shoulder module with an IMU. However, this change will dramatically raise the cost of the system. Except for the singularity, the OLE-based module can accurately capture individual joint angle and all the arm movements.

The data quality along with the sensing module's low cost, compact size, improved versatility, and wearability suggest that our system may be used for numerous applications in home-based rehabilitation. The ergonomic design of the OLE-based system allows patients to do it themselves and use the system for their personal rehabilitation session with comfort. The ease of system setting, calibration, and use would minimize technical issues that users may face in unsupervised home environment. In addition, the OLE-based system can be used with virtual-reality software to provide visual feedback, avoid boredom, and help users to personalize the rehabilitation therapy and self-assess the progress of recovery.

VIII. CONCLUSION

We have presented the design of the OLE-based system for the function of capturing human arm motion. The encoder counts the number of engraved lines on a reflective strip to track the travel distance. If worn properly on human body, the recorded distance can be converted to joint angles. Various experiments were conducted to test the performance of the OLE in tracking motions. In the off-body comparison test, OLE showed the correlation coefficient of 0.999 and rms error of 1.2 with respect to PowerCube. In the *in situ* test, compared with Goniometer, OLE performs the correlation coefficient of 0.990 and rms error of 3.8°; compared with ShapeWrap, OLE perform the correlation coefficient of 0.992 and rms error of 3.1°. Hence, the performance of the OLE is comparable to that of the commercial motion capture systems.

Three sensing nodes were formed into a sensor network through CAN bus for capturing free motion of human arm. The sensor network was attached on the arm and evaluated for repeatability and reliability of the system. We designed a protocol to test the sensor property by asking subjects to perform an

arm-reaching task. We can discriminate among different types of joints' activities. The average error range is 2.819°. In addition, the average SD is 0.697°. Reliability analysis shows high ICC values within 0.959–0.975, with an overall average of 0.967. These tests confirm our system's ability to perform and maintain its functions in routine circumstances, with different biometric subjects.

The OLE-based system would find wide range of applications in the field of rehabilitation. In fact, we have been cooperating with Tan Tock Seng Hospital (Singapore) to develop a motion capture device based on this paper's work for monitoring and assessing stroke rehabilitation processes.

ACKNOWLEDGMENT

The authors would like to thank K. Y. Lim, Y. K. Goh, and W. Dong for their contributions to the project.

REFERENCES

[1] E. Taub, N. E. Miller, T. A. Novack, E. W. Cook 3rd, W. C. Fleming, C. S. Nepomuceno, J. S. Connell, and J. E. Crago, "Technique to improve chronic motor deficit after stroke," *Arch. Phys. Med. Rehabil.*, vol. 74, pp. 347–354, 1993.

[2] M. Cirstea and M. Levin, "Compensatory strategies for reaching in stroke," *Brain*, vol. 123, pp. 940–953, 2000.

[3] B. Rohrer, S. Fasoli, H. I. Krebs, R. Hughes, B. Volpe, W. R. Frontera, J. Stein, and N. Hogan, "Movement smoothness changes during stroke recovery," *J. Neurosci.*, vol. 22, pp. 8297–8304, 2002.

[4] R. Dickstein, Y. Heffes, Y. Laufer, N. Abulaffio, and E. L. Shabtai, "Repetitive practice of a single joint movement for enhancing elbow function in hemi-paretic patients," *Perceptual Motor Skills*, vol. 85, pp. 771–785, 1997.

[5] G. Alon, A. F. Levitt, and P. A. McCarthy, "Functional electrical stimulation enhancement of upper extremity functional recovery during stroke rehabilitation: A pilot study," *Neurorehabil. Neural Repair*, vol. 21, pp. 207–215, 2007.

[6] E. Taub, G. Uswatte, and T. Elbert, "New treatments in neurorehabilitation founded on basic research," *Nat. Rev. Neurosci.*, vol. 3, no. 3, pp. 228–236, 2002.

[7] C. Jadhav, P. Nair, and V. Krovi, "Individualized interactive home-based haptic telerehabilitation," *IEEE Multimedia*, vol. 13, no. 3, pp. 2–9, Jul.–Sep. 2006.

[8] G. Burdea and P. Coiffet, *Virtual Reality Technology*. New York: Wiley, 1994.

[9] K. Kong and M. Tomizuka, "Control of exoskeletons inspired by fictitious gain in human model," *IEEE/ASME Trans. Mechatron.*, vol. 14, no. 6, pp. 689–698, Dec. 2009.

[10] N. Arai and H. Shinada, "Optical linear encoder" U.S. Patent 4 667 099, May 19, 1987.

[11] K. Y. Lim, F. Y. K. Goh, W. Dong, K. D. Nguyen, I.-M. Chen, S. H. Yeo, H. B. L. Duh, and C. G. Kim, "A wearable, self-calibrating, wireless sensor network for body motion processing," in *Proc. IEEE Int. Conf. Robot. Autom.*, California, May 2008, pp. 1017–1022.

[12] W. Dong, K. Y. Lim, F. Y. K. Goh, K. D. Nguyen, I.-M. Chen, S. H. Yeo, and H. B. L. Duh, "A low-cost motion tracker and its error analysis," in *Proc. IEEE Int. Conf. Robot. Autom.*, May 2008, pp. 311–316.

[13] G. Welch and E. Foxlin, "Motion tracking: No silver bullet, but a respectable arsenal," *IEEE Comput. Graph. Appl.*, vol. 22, no. 6, pp. 24–38, Nov./Dec. 2002.

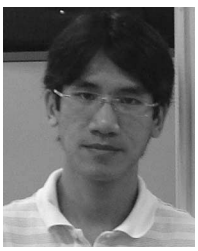

Kim Doang Nguyen (S'07) received the B.E. degree in mechanical engineering from Nanyang Technological University (NTU), Singapore, in 2007.

Since 2007, he has been a Research Staff Member in the School of Mechanical and Aerospace Engineering, NTU. His research interests include motion planning, human–robot interaction, biomechanics, neural prosthetics, and brain–machine interface.

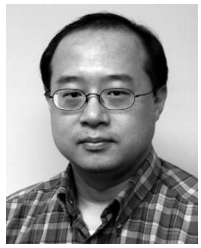

I-Ming Chen (M'95–SM'06) received the B.S. degree from National Taiwan University, Taipei, China, in 1986, and the M.S. and Ph.D. degrees from California Institute of Technology, Pasadena, in 1989 and 1994, respectively.

He was a JSPS Visiting Scholar at Kyoto University, Kyoto, Japan in 1999. He was a Visiting Scholar in the Department of Mechanical Engineering, Massachusetts Institute of Technology (MIT), Cambridge, in 2004. Since 1995, he has been with the School of Mechanical and Aerospace Engineering, Nanyang Technological University, Singapore, where he is currently the Director of the Intelligent Systems Center. He is a member of the Editorial Boards of *Mechanism and Machine Theory*, and *Robotica* and an Associate Editor-in-Chief of *Frontier of Mechanical Engineering* (Springer-Verlag). His research interests include wearable sensors, human–robot interaction, reconfigurable automation, parallel kinematics machines, biomorphic underwater robots, and smart material-based actuators. He has authored or coauthored more than 200 papers in refereed international journals and conference proceedings, as well as book chapters.

Dr. Chen is a member of the Editorial Board of the IEEE TRANSACTIONS ON ROBOTICS, and served in the same capacity for the IEEE/ASME TRANSACTIONS ON MECHATRONICS from 2003 to 2009. He was General Chairman of 2006 IEEE Conference on Cybernetics, Intelligent Systems, and Robotics and General Chairman of the 2009 IEEE/ASME International Conference on Advanced Intelligent Mechatronics. He was a Fellow of the Singapore-MIT Alliance from 2003 to 2007.

Zhiqiang Luo (M'08) received the B.S. and M.S. degrees from Beijing Jiaotong University, Beijing, China, in 2000 and 2003, respectively, and the Ph.D. degree in human factors and ergonomics from Nanyang Technological University (NTU), Singapore, in 2008.

He is currently a Research Fellow in the School of Mechanical and Aerospace Engineering, NTU. His research interests include human–computer interaction, human factors, ergonomics, and interaction between real and virtual worlds through motion communication.

Song Huat Yeo received the B.S. and Ph.D. degrees from the University of Birmingham, Birmingham, U.K., in 1983 and 1987, respectively.

Since 1992, he has been with the School of Mechanical and Aerospace Engineering (MAE), Nanyang Technological University (NTU), Singapore, where he is currently an Associate Professor. His research interests include mechanics of gripping, kinematics of parallel robots and expert systems cable-driven mechanisms, synthesis of mechanisms, wearable haptics devices, and kinematics of reconfigurable robots.

Dr. S. H. Yeo was the recipient of the MAE Teacher of the Year Award in 1998.

Henry Been-Lirn Duh (SM'09) received the B.S. degree from National Chengchi University, the M.S. degree from National Cheng Kung University, Tainan City, China, in 1994, and the M.S. and Ph.D. degrees in industrial engineering from the University of Washington, in 1999 and 2002, respectively.

He is currently the Deputy Director (Research) of the KEIO–NUS Connective Ubiquitous Technology for Embodiments Center and an Assistant Professor in the Department of Electrical and Computer Engineering and Interactive and Digital Media Institute, National University of Singapore. His research interests include user experiences, interaction design, and game effects in advanced display and mobile systems.

Dr. Duh is the Singapore Representative of the International Federation for Information Processing Technical Committee 13: Human–Computer Interaction and Chairman of the Association for Computing Machinery Singapore Chapter.